A Component-Based Approach to Hand Verification

Gholamreza Amayeh and George Bebis and Ali Erol and Mircea Nicolescu
Computer Vision Laboratory, University of Nevada, Reno, NV 89557
{amayeh, bebis, aerol, mircea}@cse.unr.edu

Abstract

This paper describes a novel hand-based verification system based on palm-finger segmentation and fusion. The proposed system operates on 2D hand images acquired by placing the hand on a planar lighting table without any guidance pegs. The segmentation of the palm and the fingers is performed without requiring the extraction of any landmark points on the hand. First, the hand is segmented from the forearm using a robust, iterative methodology based on morphological operators. Then, the hand is segmented into six regions corresponding to the palm and the fingers using morphological operators again. The geometry of each component of the hand is represented using high order Zernike moments which are computed using an efficient methodology. Finally, verification is performed by fusing information from different parts of the hand. The proposed system has been evaluated on a database of 101 subjects illustrating high accuracy and robustness. Comparisons with competitive approaches that use the whole hand illustrate the superiority of the proposed, component-based, approach both in terms of accuracy and robustness. Qualitative comparisons with state of the art systems illustrate that the proposed system has comparable or better performance.

1. Introduction

Hand-based authentication is among the oldest live biometrics-based authentication modalities. The existence of several commercial hand-based verification systems and patents indicate the effectiveness of this type of biometric. Hand-based verification systems are usually employed in small-scale person authentication applications due to the fact that geometric features of the hand are not as distinctive as fingerprint or iris features.

There are several reasons for developing hand-based authentication systems. First, hand shape can be easily captured in a relatively user friendly manner by using conventional CCD cameras. Second, this technology is more acceptable by the public in daily life mainly because it lacks a close connection to forensic applications. Finally, there has been some interest lately in fusing different biometrics to increase system performance [21, 14]. The ease of use and acceptability of hand-based biometrics make hand shape a good candidate in these heterogeneous systems.

The majority of hand-based verification systems using geometric measurements are based on research limited to considerably old patents [10] and commercial products. In these systems, the user is asked to place his hand on a surface and align it with the help of some guidance pegs on the surface. Enhancing the ease of use and/or recognition accuracy of these systems has drawn some attention only recently. There are two main research directions: (i) designing more convenient, peg-free systems and (ii) extracting more powerful features to improve accuracy and robustness.

Several studies have reported that peg-based alignment is not very satisfactory and represents in some cases a considerable source of failure [22, 11]. Although peg removal provides a solution to reduce user inconvenience, it also raises more challenging research problems due to the increase in intra-class variance due to inaccuracies in feature extraction. Nevertheless, most recent studies have concentrated on the design of peg-free systems. Extracting extremities of the hand contour, such as finger valleys and finger tips, is usually the first processing step in these systems. An exception is the approach of [11] which uses the whole hand silhouette contour for alignment and matching.

Kumar et. al [14] used palm-print and hand geometric features. In their approach, the extremities of the hand contour were used to measure finger length and palm width. Ma et. al [17] used these landmarks as control points to fit B-spline curves on fingers. Sanchez-Reillo et al. [23, 22] proposed a new, richer set of geometric features and investigated the use of multiple templates per subject. Recently, Yoruk et. al. [27] introduced a more accurate and detailed representation of the hand using the Hausdorff distance of the hand contour, and Independent Component Analysis (ICA). Their approach requires registering the silhouettes of the hand images using the locations of fingertips and valleys.

A different approach, involving the reconstruction of the 3D surface of the hand, was proposed in [25]. In their approach, Woodard et. al [25] used a range sensor to reconstruct the dorsal part of the hand. Local shape index values of the fingers were used as features in matching. In a related study, Lay et. al. [16] projected a parallel grating onto the dorsal part of the hand to extract features that indirectly capture 3D shape information.

In this paper, we propose a novel, peg-free approach to hand-based verification which does not depend on the position and orientation of the hand or finger movement. There are two key ideas behind the proposed approach. First, decomposing the hand image in several regions corresponding to the palm and fingers. Second, fusing information from different parts of the hand to improve accuracy and robustness. This work builds upon our earlier work [2] where the geometry of the whole hand was represented using high order Zernike moments. Although Zernike moments can tolerate certain degree of finger movement (e.g., around six degrees rotation about the axis being perpendicular to the joint of the finger with the palm), they are quite sensitive to big finger movements. Moreover, Zernike moments cannot tolerate well situations where the hand is bent at the wrist. As we show in this paper, palm-finger segmentation can alleviate these problems while improving accuracy and robustness.

Our approach operates on 2D hand images acquired by placing the hand on a planar lighting table without any guidance pegs. To simplify finger segmentation, we require that the subjects stretch their hand prior to placing it on the lighting table in order to avoid touching fingers. No other restriction was imposed on the subjects. An important characteristic of our approach is that it does not require the extraction of any landmark points, a process which is prone to errors. In contrast, we segment the hand image in different regions using a robust methodology based on morphological operators. Then, instead of representing the hand using explicit geometrical measurements, we represent the geometry of each part of the hand implicitly using region-based features (i.e., Zernike moments). The approach adopted here leads to significant computational savings. In contrast to [2], however, which requires employing very high order Zernike moments (i.e., up to 70) to represent the geometry of the hand, the geometry of the fingers and the palm can be represented using relatively low order moments (i.e., up to 20) which can be computed both faster and more accurately.

Although fusing information from different biometric modalities (i.e., face, fingerprint, hand) has received significant attention lately, fusing information from different parts of the same biometric is less common. For example, Ross and Govindarajan [20] have reported a feature level fusion scheme using hand and face features. Kumar and Zhang [15] have investigated feature selection of hand shape and palm print features. Cheung et al. [5] have proposed a two level fusion strategy for multimodal biometric verification. Jiang and Su [12] have investigated fusing faces and fingerprints to improve verification accuracy.

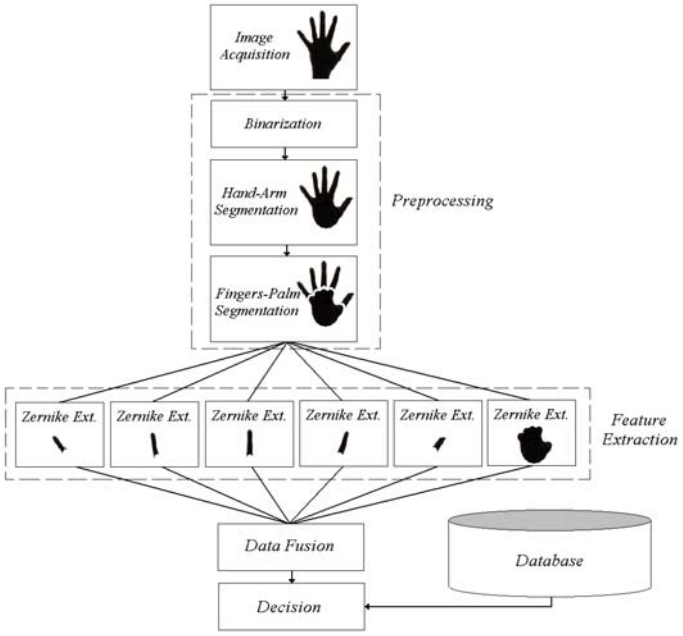

Figure 1. Block diagram of proposed system.

Our approach is mostly related to component-based approaches which have shown promising results in various object detection and recognition tasks [1][24] including face detection/recognition [9] and person detection [18]. The main idea in these approaches is representing an object in terms of its parts and their geometrical relationships. Among them, the closest approach to ours is the face recognition system reported in [9] where information from different parts of the face were fused together to improve recognition performance. In that study, fusion was implemented at the feature level (i.e., combining all the features in one vector and feeding it to a Support Vector Machine (SVM) [6] classifier). In this paper, we have investigated several different fusion strategies including feature, score and decision level fusion.

The rest of the paper is organized as follows: in Section 2, we present an overview of the proposed system. Section 3 contains the details of preprocessing and segmentation. In Section 4, we discuss the feature extraction scheme. Our fusion strategies are presented in Section 5 while our experimental results and comparisons are presented in Section 6. Finally, Section 7 contains our conclusions and plans for future work.

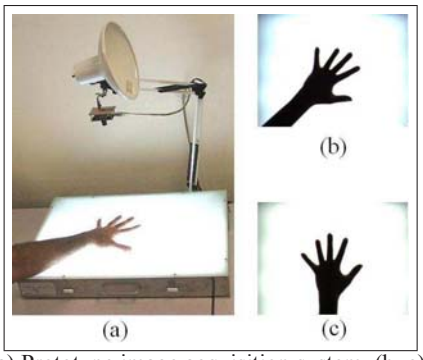

Figure 2. (a) Prototype image acquisition system, (b, c) images of the same hand.

2. System Overview

Figure 1 shows the main stages of our proposed system. The image acquisition system, shown in Figure 2(a)) consists of a VGA resolution CCD camera and a planar lighting table, which forms the surface for placing the hand. The direction of the camera is perpendicular to the lighting table. The camera has been calibrated to remove lens distortion. Figures 2 (b),(c) show some sample images acquired by our system. Under this setting, a fixed threshold is sufficient to extract a binary silhouette of the hand and the arm robustly.

After image acquisition, the image acquired is binarized and goes through the segmentation module. During segmentation, the arm is separated from the hand and discarded from further processing. Then, the hand is processed to segment the palm and the fingers. Feature extraction is performed by computing the Zernike moments of each part of the hand independently. The resulting representation is invariant to translation, rotation and scaling transformations. Finally, verification is performed by fusing information from different parts of the hand. In our current implementation, we employ multiple enrollment templates per subject and compute similarity scores using the minimum distance between a query image and the templates of the subject.

3. Preprocessing

This stage includes the binarization of the acquired image and its segmentation into different regions corresponding to the forearm, hand, palm, and fingers. Our current setting yields very high quality images, which are almost free of shadows and noise. As a result, binarization can be performed using a single threshold. To separate the forearm from the hand, first we detect the palm by finding the largest circle that can be prescribed inside the hand-arm silhouette. To segment the hand, we take the intersection of the forearm with the circle's boundary. To segment the fingers from the palm, we filter out the fingers first using morphological closing [7]; then, the palm is subtracted from the hand silhouette to segment the fingers. It should be mentioned that segmenting the hand into different regions could be done probably faster by detecting certain landmarks on the hand silhouette, however, such an approach would be more prone to segmentation errors. Details of these steps are provided below.

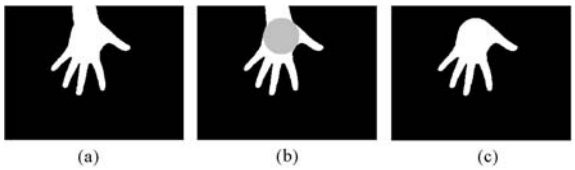

Figure 3. (a) Binarized image, (b) largest circle inside of hand-arm silhouette (c) segmented hand silhouette.

3.1. Hand-Forearm Segmentation

The binary silhouette obtained during image acquisition is the union of the hand with the forearm. The forearm does not have many distinctive features while its silhouette, at different acquisition sessions, is not expected to be the same due to clothing and freedom in hand placement (see Figures 2(b),(c)). To segment the forearm, we assume that the user is not wearing very loose clothing on the arm. Under this assumption, the palm becomes the thicker region of the silhouette, which enables us to detect it by finding the largest circle inside the silhouette. We use morphological closing based on a circular structuring element [7] to find the largest circle. The algorithm can be summarized as follows:

1. Initialize a circular structuring element D with a very large radius R
2. Apply closing operator on the image using D
3. If the output is an empty image then set R:=R-1 and go to 2. Otherwise the resulting image corresponds to the largest circle inside the silhouette.

Figure 3(b) shows the output of the algorithm above on a sample image. Once the largest circle is found, the forearm is segmented by detecting its intersection with the circle and the boundary of the image. Figure 3(c) shows the resulting silhouette after discarding the forearm region.

3.2. Palm-Finger Segmentation

During image acquisition, we asked the subjects to stretch their hand in order to avoid touching fingers, however, finger motion was unavoidable. Figure 4(a) shows two samples collected from the same user. As it can be observed, the angles between fingers can change a lot between samples. Deformations of the hand silhouette due to finger movement can affect the Zernike moments significantly as

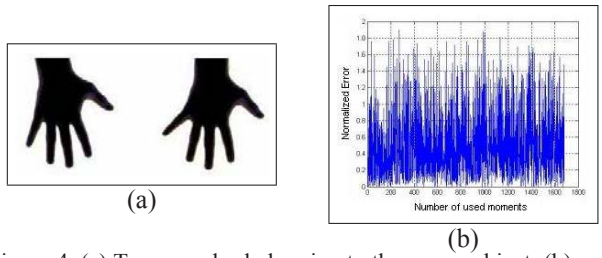

Figure 4. (a) Two samples belonging to the same subject; (b) normalized Zernike moment differences corresponding to these samples.

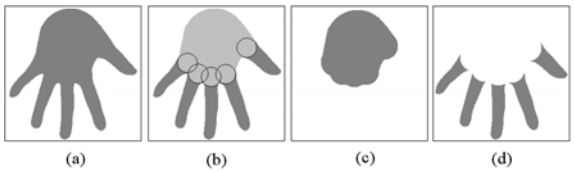

Figure 5. (a) Hand silhouette, (b) morphological closing, (c) the result of closing and (d) the result of subtracting the palm from the hand silhouette.

shown in Figure 4(b). To allow for finger movement, the fingers and the palm would need to be segmented and processed separately.

The processing steps of the finger segmentation module are shown in Figure 5. First, a morphological closing operator based on a circular disk is applied on the hand image as shown in Figure 5(a). The radius of the structuring element was experimentally set to 25 pixels (i.e., making it thicker than the widest finger in our database). The closing operation filters out the fingers from the silhouette as shown in Figure 5(b) and (c). The remaining part of the silhouette corresponds to the palm, which is subtracted from the hand image to obtain the finger segments shown in Figure 5(d).

To identify each of the fingers quickly, we assume that hand rotations are less than 45 degrees. In our prototype system, larger rotations would require purposeful, unnatural efforts from the user. Handling larger rotations can be handled by using additional information such as the length, width, aspect ratio, and area of each finger. To extract each finger region and the palm, we use connected components [8].

3.3. Post-processing of finger regions

A closer examination of the segmentation results shown in Figure 5(d) reveal that the segmented fingers have sharp tails at the locations of separation from the palm. In the case of the little, point and thumb fingers, there might be significant differences in the length of these tails as illustrated in Figure 6(a) where different samples of the same subject are shown. The variation in the length of the tails can introduce important errors in the computation of the Zernike moments. To keep these errors as low as possible, we apply an additional morphological closing on each finger as shown in Figure 6(b). The structuring element in this case is a simple 4 by 4 square whose elements are equal to one. Table 1 illustrates the effect of this step by showing the normalized distances between the pairs of fingers shown in Figure 6.

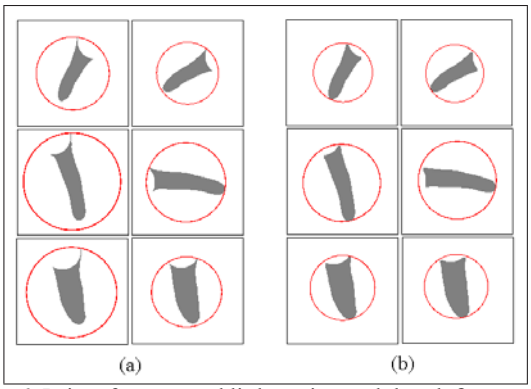

Figure 6. Pairs of segmented little, point, and thumb fingers. Each pair corresponds to two different samples of the same subject. (a) before applying the additional step, and (b) after applying the additional step.

Table 1. The effect of the extra morphological closing operator on the normalized distances between the Zernike moments (up to order 20) of the segmented finger pairs before (Figure 6a) and after (Figure 6b) the extra step.

Pair of Fingers	d_{before}	d_{after}
Little	0.5904	0.0901
Point	0.7881	0.1135
Thumb	0.7424	0.1253

It should be mentioned that an alternative solution to segment the fingers from palm is by detecting certain landmark points on the hand such as fingertips and valleys. This solution, however, would much more prone to errors due to inaccuracies in landmark detection and extraction.

4. Feature Extraction

To represent the geometry of the palm and the fingers, we use Zernike moments [13]. When using Zernike moments, one has to deal with several practical issues including computational cost of high-order Zernike moments and lack of accuracy due to limited numerical precision. In this work, we employ an improved algorithm, proposed in one of our earlier works [3], which speeds up computations by exploiting some recursive relations in the computation of the Zernike moments and by using look-up tables. Accuracy can be achieved using arbitrary precision arithmetic.

A crucial parameter here is determining the maximum Zernike moment order to represent the geometry of different parts of the hand. Capturing the details of the input

image usually requires very high orders. On the other hand, arbitrarily high order moments are not expected to be accurate and useful for recognition. We used the average reconstruction error on a large number of palm and finger images to decide the maximum order that would be useful in the context of our application. By analyzing the reconstruction error, the maximum order was set to 20 for the fingers and to 30 for the palm. It should be mentioned that the same analysis was used to represent the geometry of the whole hand in [2], yielding an order of 70. Clearly, decomposing the hand in different parts improves the processing speed of the system considerably.

5. Fusion

This module fuses information from different parts of the hand to improve verification accuracy and robustness. In general, fusion can be performed at different levels. In this paper, we have experimented with three different fusion strategies: *feature level, score level, and decision level*.

5.0.1 Feature Level Fusion Using Principal Component Analysis

The use of Principal Components Analysis (PCA) [**?**] for feature level fusion is quite popular. In this case, the feature vectors of the palm and the fingers are combined into a single feature vector. Then, PCA is applied to map them into a lower dimensional space. Essentially, each PCA feature represents a linear combination of the original features.

5.0.2 Score Level Fusion Using Weighted Sum

The weighted sum rule has been extensively investigated in the literature and it is the most straightforward fusion strategy at the score level. In this case, the matching scores between pairs of fingers and pairs of palms between query and template hands are combined into a single score using a weighted sum as follow:

$$S(Q,T) = \sum_{i=1}^{6} \alpha_i S(Q_i, T_i) \tag{1}$$

where S is the similarity measure (e.g., distance) between the query Q and the template T. Q_i, and T_i represent the i-th parts of the query and template. In our system, the first five parts correspond to the little, ring, middle, point and thumb fingers while the sixth part corresponds to the palm. The parameters α_i are the weights associated with the i-th part of the hand which need to satisfy the following constraint:

$$\sum_{i=1}^{6} \alpha_i = 1 \tag{2}$$

The main issue with this method is determining a set of appropriate values for the weights. Here, we determined the weight values experimentally by investigating the discrimination power of each part of the hand. Specifically, we performed a number experiments using each part of the hand separately for verification purposes. By measuring the Equal Error Rate (EER) for each part of the hand, we found that the certain parts of the hand have higher discrimination power than others. For example, the index and the thumb fingers had the highest and lowest discrimination power correspondingly. This is mainly because it is more difficult to segment the thumb very accurately due to higher motion flexibility. Based on these observations, we assigned the weight for each part according to its discrimination power. The best results, reported in our experimental section, were obtained using the following weight values: w_1 = 0.5 / 12 (little finger), w_2 = 2.5 / 12 (ring finger), w_3 = 3.0 / 12 (middle finger), w_4 = 4.5 / 12 (index finger), w_5 = 0.5 / 12 (thumb), and w_6 = 1.0 / 12 (palm).

5.0.3 Decision Level Fusion Using Majority Voting

Majority voting is among the most straightforward decision level fusion strategies. In this case, the final decision is based on the output results of several matchers. In the context of hand verification, we verify the identity of a subject using each part of the hand (i.e., fingers and palm) separately. Then, if three or more parts of the hand support the same verification result, we accept this result as a correct verification; otherwise, we reject the subject.

6. Experimental Results

In order to evaluate our system, we have hand collected data from 101 people of different age, sex and ethnicity. For each subject, we collected 10 images of his/her right hand during the same session. Subjects were asked to stretch their hand and place it inside a square area drawn on the surface of the lighting table; however, no other restrictions were imposed on the subjects. To capture different samples, subjects were asked to remove their hand from the lighting table, relax it for a few seconds, and then place it back again. As a result, finger movement was unavoidable as shown in Figure 4(a).

To calculate the distance between a query hand Q and the template hands T_i of an individual in the database, we compute all Euclidean distances between the query and the templates and take the minimum distance:

$$D = arg_i min\{||Q - T_i||\}, i = 1, .., k \tag{3}$$

where k corresponds to the number of templates. If the minimum distance is below a threshold, then verification is considered successful; otherwise the subject is rejected.

In the following subsections, we report our evaluation results based on the proposed hand-based verification system. First, we compare the different fusion strategies discussed earlier. Then, we illustrate the effectiveness of the hand decomposition scheme by comparing it with the approach of [2] where the whole hand is used for verification without segmentation.

6.1. Verification using hand decomposition and fusion

For evaluation purposes, we used different numbers of samples (i.e., 3,4, and 5) for each subject as enrollment templates. To capture the effect of template selection on overall system performance, we repeated each experiment 30 times, each time choosing the enrollment templates randomly. The remaining samples were used to construct matching and non-matching sets to estimate False Acceptance Rate (FAR) and False Reject Rate (FRR).

In feature level fusion, the feature vectors of each part of the hand were combined into a single feature vector yielding 861 features. Using PCA and keeping 99.9% of the information in the data yields vectors containing between 72 and 81 features. Figures 7, 8, 9 show the average ROC curves of each fusion strategy using different template sizes. Table 2 compares the fusion strategies in terms of EER as well as the mean and the standard division of TAR when $FAR = 0.1\%$. As it can be observed, all fusion methods improved system performance so that TAR is more than 99.4% when FAR is more than 0.1%. Overall, majority voting had the best performance among the three fusion strategies considered here. PCA had the lowest performance, however, using PCA reduces the size of templates by more than 10 times.

To further investigate the performance of our system, we have performed a qualitative comparison of its error rate with those reported in the literature. It should be mentioned that since there is no standard acquisition method and, as a result, no benchmark databases, quantitative comparisons of different systems are not completely fair and should be taken as indicative only and not conclusive. Our database size is comparable to most of the systems reported here and our error rates are better even to the ones reported on much smaller databases.

Yoruk et al. [27] have reported a 1.79% EER using 458×2 (# of people $\times$ # of samples per person) images as enrolment set and 458×1 as test set. Xiong et al. [26] have reached a 2.41% EER using 108×1 images as enrolment set and 108×4 as test set. Ma et al [17] have reported a 5% error rate using 20×1 images as enrolment set and 20×5 as test set. Reillo et al. [23] Show less than 5% EER using 20×5 images as enrolment set and 20×5 as test set. Bulatov et al. [4] have reported a $TAR = 97\%$ when $FAR = 1\%$ using 70×5 images as enrolment set and 70×5 as test set. Ribaric et al. [19] have reported a $TAR = 1.1\%$ when $FAR = 1.22\%$ on a database which includes 130×1 images as enrolment set and 130×4 as test set. Their approach fuses information from the hand and the palm print using a weighted sum rule. Finally, Kumar et al [14] have fused hand geometry and palm print features at the decision level, reporting a $TAR = 92\%$ when $FAR = 1\%$ using 100×5 images as enrolment set and 100×5 as test set.

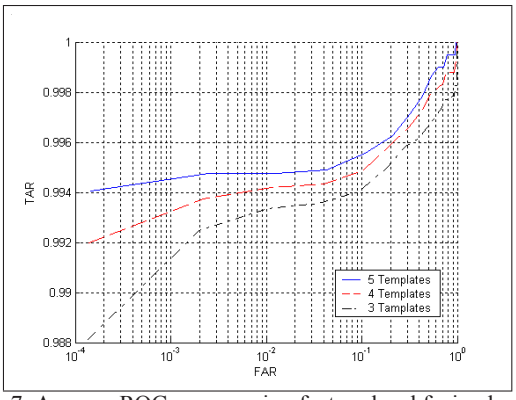

Figure 7. Average ROC curves using feature level fusion based on PCA using 3, 4, and 5 templates per subject. The experiment was performed 30 times using a different training set each time.

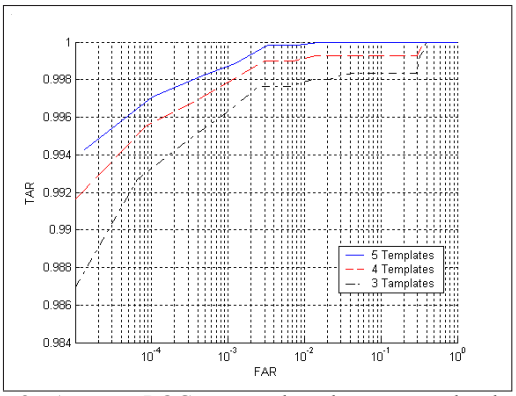

Figure 8. Average ROC curves based on score level fusion (weighted sum) using 3, 4, and 5 templates per subject. The experiment was performed 30 times using a different training set each time.

Table 2. Comparison of different fusion techniques using 5 templates per subject as enrolment size.

Method	PCA	Weighted Sum	Majority Voting
$\overline{EER}(\%)$	0.523	0.119	0.044
$\overline{TAR}(\%)$ (FAR=0.1%)	99.47	99.86	99.98
$\sigma_{TAR}(\%)$ (FAR=0.1%)	0.231	0.119	0.059

6.2. Verification using whole hand

For comparison purposes, we have compared our system with the one reported in [2] where the whole hand is used

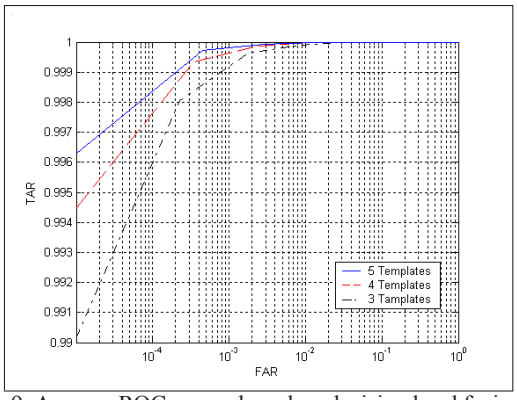

Figure 9. Average ROC curves based on decision level fusion (majority voting) using 3, 4, and 5 templates per subject. The experiment was performed 30 times using a different training set each time.

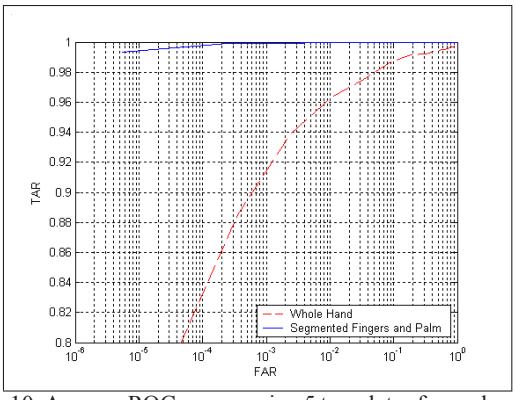

Figure 10. Average ROC curves using 5 templates for each subject; the solid curve corresponds to the whole hand while the dashed one corresponds to the weighted sum of the finger and palm features. The experiment was performed 30 times using a different training set each time.

for verification without segmentation. In this case, only the arm is segmented from the rest of the hand and hand geometry is represented by computing the Zernike moments of the whole hand. As mentioned earlier, in the case of the whole hand, we need to compute Zernike moments up to order 70 which is very time consuming. On the other hand, the palm and the fingers require much lower orders (i.e. up to order 20 and 30 for fingers and palm respectively). It is worth mentioning that it is taking about 6 minutes to compute the Zernike moments of the whole hand silhouette up to order 70, while it is only taking 35 seconds to compute the Zernike moments of the fingers and palm up to order 20 and 30 respectively.

Figure 10 shows the ROC curves of the two systems. In both cases, we used 5 enrollment templates. As it can observed, finger segmentation improves performance to a great extent. For example, when FAR=1%, TAR increases from 96.06% to 100% when employing palm-finger segmentation and fusion. The reason for this, as mentioned in 3.2, is because finger *segmentation* eliminates the effect of finger movements which can affect Zernike moments significantly in all orders (i.e., see Fig 4).

6.3. System Performance Over Time

In this section, we report preliminary results to illustrate the performance of majority voting over large lapses of time. In this context, we recorded 10 new samples from 20 subjects of the 101 subjects after a period of 9 months (i.e., 200 images). These samples were used to test the performance of our system when there is a substantial passage time between the acquisition of the template and test images. In a similar manner as before, we repeated each experiment 30 times using 3, 4, and 5 samples from our initial data collection as enrolment templates. To keep results consistent, we used exactly the same enrolment templates in each experiment as in our previous experiments. Fig. 11

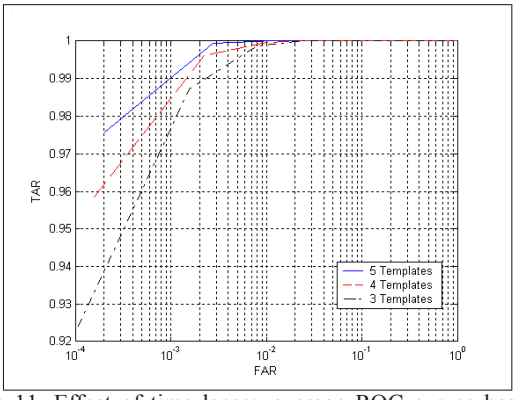

Figure 11. Effect of time lapse: average ROC curves based on decision level fusion (majority voting) using 3, 4, and 5 templates per subject. The experiment was performed 30 times using the same enrollment templates as in the previous experiments. For testing, we used 200 images from 20 of the 101 subjects, taken 9 months later.

shows the average ROC curves obtained in this case. As it can be observed by comparing Fig. 11 with Fig. 9, there is a small deterioration in system performance over time, however, this is quite reasonable and acceptable.

7. Conclusion

We have presented a component-based hand verification system using palm-finger segmentation and fusion. The proposed method has certain advantages including that it is peg-free, it does require the extraction of any landmark points, and it is not affected by the orientation and position of the hand or finger movement. The only restriction imposed by our system is that the used must present his hand in a stretched configuration to avoid touching figures. Qualitative comparisons between our system and other systems reported in the literature indicate that our system performs

comparable or better.

Our system is still under development and further work is required to improve its performance. First of all, we plan to investigate the idea of combining multiple templates into a single, "super-template", to reduce memory requirements but also build more accurate models for each individual. In particular, we plan to investigate ways to update the "super-template" over time (i.e., template "aging") to maintain system performance. Second, we plan to increase the size of the database in order to perform larger scale experiments and obtain more accurate error estimates. Moreover, we plan to test more systematically the robustness of the method when there is substantial passage time between the template and test images. Finally, we plan to compare our technique with other techniques using the same datasets to reach more useful conclusions.

References

[1] S. Agarwal, A. Awan, and D. Roth. Learning to detect objects in images via a sparse, part-based representation. *IEEE Transactions on Pattern Analysis and Machine Intelligence.*, 26(11):1475– 1490, 2004.

[2] G. Amayeh, G. Bebis, A. Erol, and M. Nicolescu. Peg-free hand shape verification using high order zernike moments. *IEEE Computer Society Workshop on Multi-modal Biometrics, New York City, NY*, June 17-18, 2006.

[3] G. Amayeh, A. Erol, G. Bebis, and M. Nicolescu. Accurate and efficient computation of high order zernike moments. *First International Symposium on Visual Computing, ISVC 2005, Lake Tahoe, NV, USA*, pages 462–469, December 2005.

[4] Y. Bulatov, S. Jambawalikar, P. Kumar, and S. Sethia. Hand recognition using geometric classifiers. *ICBA'04, Hong Kong, China*, pages 753–759, July 2004.

[5] M. Cheung, M. Mak, and S. Kung. A two level fusion approach to multimodal biometrics verification. *IEEE International Conference on Acoustics, Speech, and Signal Processing,(ICASSP '05).*, 5:485– 488, 18-23 March 2005.

[6] R. Duda, P. Hart, and D. Stork. *Pattern Classification*. 2nd edition, 2000.

[7] R. C. Gonzalez and R. E. Woods. *Digital Image Processing*. Prentice-Hall, 2002.

[8] R. M. Haralock and L. G. Shapiro. *Computer and Robot Vision*. Addison-Wesley Longman Publishing Co., Inc., Boston, MA, USA, 1991.

[9] B. Heisele. Visual object recognition with supervised learning. *IEEE Intelligent Systems.*, pages 38– 42, May/June 2003.

[10] A. K. Jain, R. Bolle, and S. Pankanti. *Biometrics: personal identification in networked society*. Kluwer Academic Publishers, 1999.

[11] A. K. Jain and N. Duta. Deformable matching of hand shapes for verification. *Proc. IEEE Int. Conf. on Image processing, Kobe, Japan*, pages 857–861, October 1999.

[12] C. Jiang and G. Su. Information fusion in face and fingerprint identity verification system. *the Third International Conference on Machine Learning and Cybernetics*, pages 3529–3535, 26-29 Aug 2004.

[13] A. Khotanzad and Y. H. Hong. Invariant image recognition by zernike moments. *IEEE Transactions on Pattern Analysis and Machine Intelligence*, 12:489 – 498, 1990.

[14] A. Kumar, D. C. M. Wong, H. C. Shen, and A. K. Jain. Personal verification using palmprint and hand geometry biometric. *Time-Varying Image Processing and Moving Object Recognition, Guildford, UK*, pages 668–678, June 2003.

[15] A. Kumar and D. Zhang. Personal recognition using hand shape and texture. *IEEE Transactions on Image Processing*, 15:2454– 2461, Aug. 2006.

[16] Y. L. Lay. Hand shape recognition. *Optics and Laser Technology*, 32(1):1–5, Feb. 2000.

[17] Y. L. Ma, F. Pollick, and W. Hewitt. Using b-spline curves for hand recognition. *Proc.of the 17th International Conference on Pattern Recognition (ICPR'04)*, 3:274–277, Aug. 2004.

[18] A. Mohan, C. Papageorgiou, and T. Poggio. Example-based object detection in images by components. *IEEE Transactions on Pattern Analysis and Machine Intelligence.*, 23(4):349– 361, 2001.

[19] S. Ribaric, D. Ribaric, and N. Pavesic. Multimodal biometric user-identification system for network-based applications. *IEE Proceedings on Vision, Image and Signal Processing*, 150, Issue 6:409–416, 15 Dec. 2003.

[20] A. Ross and R. Govindarajan. Feature level fusion using hand and face biometrics. *SPIE Conference on Biometrics Technology for Human Identification*, 5779(2):196–204, March 2005.

[21] A. Ross and A. K. Jain. Information fusion in biometrics. *Pattern Recognition Letters*, 24(13):2115–2125, 2003.

[22] R. Sanchez-Reillo. Hand geometry pattern recognition through gaussian mixture modelling. *15th International Conference on Pattern Recognition (ICPR'00)*, 2:937–940, 2000.

[23] R. Sanchez-Reillo, C. Sanchez-Avila, and A. Gonzalez-Marcos. Biometric identification through hand geometry measurements. *IEEE Transactions on Pattern Analysis and Machine Intelligence*, 22(10):1168–1171, October 2000.

[24] H. Schneiderman and T. Kanade. Object detection using the statistics of parts. *International Journal of Computer Vision.*, 56(3):151– 177, 2004.

[25] D. L. Woodard and P. J. Flynn. Personal identification utilizing finger surface features. In *CVPR*, San Diego, CA, USA, 2005.

[26] W. Xiong, C. Xu, and S. H. Ong. Peg-free human hand shape analysis and recognition. *Proc. of IEEE International Conference on Acoustics, Speech, and Signal Processing (ICASSP '05)*, 2:77–80, March 18-23 2005.

[27] E. Yoruk, E. Konukoglu, B. Sankur, and J. Darbon. Shape-based hand recognition. *IEEE Transactions on Image Processing*, 15(7):1803–1815, July 2006.